International Journal of Biological Macromolecules 104 (2017) 180–188

Contents lists available at ScienceDirect

International Journal of Biological Macromolecules

journal homepage: www.elsevier.com/locate/ijbiomac

Nicotinic acetylcholine receptor alpha 1(nAChRα1) subunit peptides as potential antiviral agents against rabies virus

Basavaraj Sajjanar[a], Kalyani Dhusia[b], Shikha Saxena[a], Vinay Joshi[c], Deepika Bisht[a], Dimpal Thakuria[d], Gundallahalli B. Manjunathareddy[e], Pramod W. Ramteke[b], Satish Kumar[a,*]

[a] Division of Veterinary Biotechnology, Indian Veterinary Research Institute, Bareilly- 243122, Uttar Pradesh, India
[b] Department of Biological Sciences, Sam Higginbottom Institute of Agriculture, Technology & Sciences, Allahabad-211007, Uttar Pradesh, India
[c] Department of Animal Biotechnology, College of Veterinary Sciences, Lala Lajapat Rai University of Veterinary & Animal Sciences, Hisar-125004, India
[d] Directorate of Cold water Fisheries, Indian Council of Agricultural Research, Anusandhan Bhawan, Bhimtal-263136, Uttarakhand, India
[e] ICAR-National Institute of Veterinary Epidemiology and Disease Informatics, Yelahanka, Bengaluru-560064, India

ARTICLE INFO

Article history:
Received 9 April 2017
Received in revised form 29 May 2017
Accepted 30 May 2017
Available online 3 June 2017

Keywords:
Antivirals
Glycoprotein peptide ligands
Rabies virus

ABSTRACT

Rabies virus (RABV) is neurotropic and infects all warm-blooded animals. The binding of the virus with host cell receptor components is critical for infection. The present study reports the interaction of nicotinic acetylcholine receptor alpha 1 (nAChRα1) peptides with the rabies virus glycoprotein (RABVG) to design potential anti-rabies agents. The nAChRα1peptide sequences from different species (bovine, human and electric fish/torpedo) were synthesized and their secondary structures were characterized using CD spectroscopy. The molecular docking analysis of nAChRα1 peptides with RABVG indicated the involvement of specific domains and their particular amino acid contributions. Bovine peptide (C-32) (docking score of 14146 kJ/mol) and torpedo peptide (T-32) (docking score of 13704 kJ/mol) were found to interact strongly with RABVG. T-32 peptides had the highest binding and inhibiting property against RABV compared to other peptide sequences. The results of both computational and experimental methods demonstrated that nAChRα1 peptides and their analogs may serve as potential antiviral agents against RABV infection.

1. Introduction

Rabies is a neglected viral zoonotic disease causing 55,000 human deaths per year worldwide [1]. Rabies is considered deadly disease because of the highest case fatality rate and is virtually lethal after the appearance of first clinical symptoms (anxiety and confusion) [2]. Currently, regular rabies vaccines and antibodies are available for standard post-exposure prophylaxis regimens and human rabies has been controlled in developed countries. However, the disease has not been completely controlled in many Asian and African countries due to socio-economic factors such as shortage and no access to existing rabies biological [3]. Certain specific murine and human anti-rabies monoclonal antibodies have been developed and tested for post-exposure treatment [4,5]. However, no significant and focused efforts have been made to develop small molecule RABV-specific antiviral agents. Development of new cost-effective broad-spectrum antiviral drugs against rabies is critical in continuing to prevent and reduce disease.

RABV belongs to the *Lyssavirus* genus of *Rhabdoviridae* family [6]. The virus is enveloped and has a single-stranded, negative-sense RNA genome. The RNA genome of the virus has five genes which code for nucleoprotein (N), phosphoprotein (P), matrix protein (M), glycoprotein (G), and a viral RNA polymerase (L) [7]. The RABVG are arranged on the surface of virus in the form of 400 trimeric spikes. It has cytoplasmic, transmembrane and ectodomains [8]. Ectodomain homotrimer spikes of the RABVG are responsible for interacting with putative host cell receptors such as nicotinic acetylcholine receptors (nAchRα), neural cell adhesion molecule (NCAM), and the p75 neurotrophin receptor (p75NTR) [9]. These interactions are critical for fusion of the virus with the host cell membrane as induced by low pH and further entry of the virus into the cells [8]. Understanding the involvement of host cell receptors interactions with RABVG is valuable to develop interventions against RABV pathogenesis. Different experiments have confirmed the interac-

* Corresponding author.
E-mail address: drsatishkumar.ivri@yahoo.co.in (S. Kumar).

http://dx.doi.org/10.1016/j.ijbiomac.2017.05.179
0141-8130/

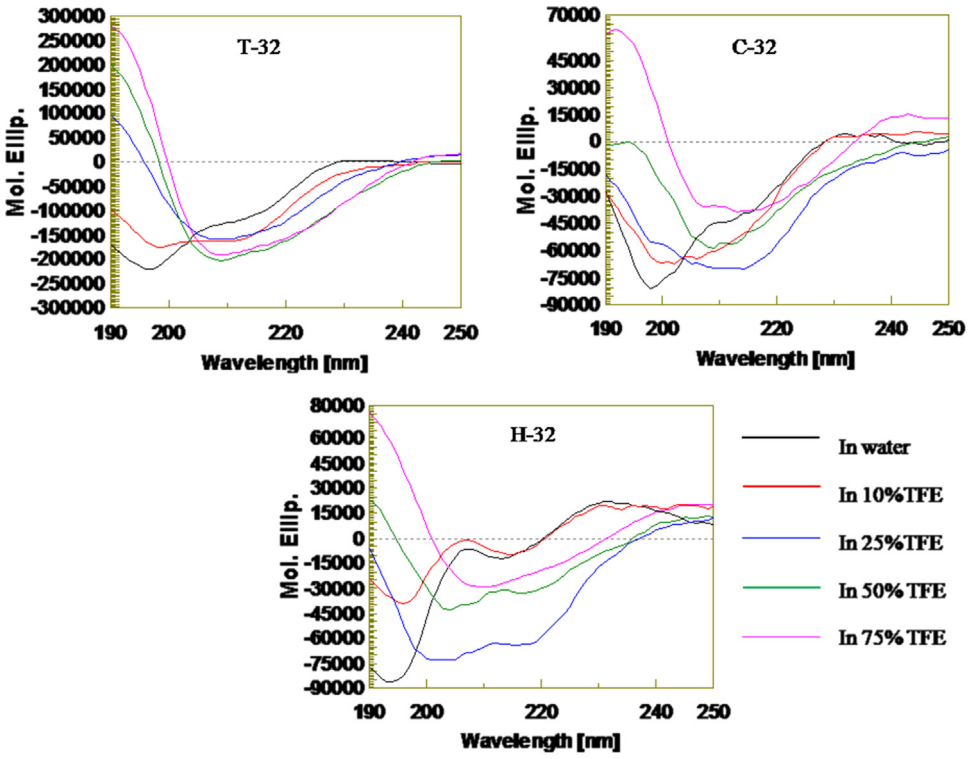

Fig. 1. CD spectra of nAChRα1-subunit peptides; T-32, C-32 and H-32 in different polar (water) and aploar (TFE) environments; in water, 10% TFE, 25% TFE, 50% TFE, 75% TFE.

tions of host cell nAChR with RABV [10]. There is a conformational similarity between the RABVG loop domain and other neurotoxins such as snake venom which is responsible for binding to the nAChR [11,12]. The nAChR at synaptic junctions and neuromuscular junctions are involved in RABV entry and spread in the nervous system [13]. The binding regions of receptors act as decoy molecules to interfere with virus infections and may be developed as potential antiviral agents. The present study was aimed to evaluate the interactions between putative host cell receptor (nAChRα1) domain peptides with the RABVG using computational and experimental methods.

2. Material methods

2.1. Peptide synthesis

Peptide synthesis was done using standard solid phase methodology with Fmoc chemistry. The nAChRα1subunit peptide sequences from 193aa to 224aa (GenBank: AAD14247.1) of bovine, human and torpedo (electric ray fish) were selected for synthesis. Rink amide MBHA resin (Nova Biochem) with loading efficiency of 0.45 was kept in DMF solvent for swelling. Activation of the first Fmoc-amino acid was done using the equivalent amount of 1-Bis (dimethylamino) methylene-1 H-benzotrizolium hexafluorophosphate (1-) 3 oxide (HBTU) and1-hydroxybenzotriazol (HOBT). The activated Fmoc-amino acid was made to react (coupling) with the resin in the presence of di-isopropyl ethylamine (DIEA) for 2 h. Coupling efficiency was monitored at each step of synthesis using Kaiser test [14]. End-capping was done with acetic anhydride followed by deprotection using piperidine (20%) to remove the Fmoc group from the first amino acid. The subsequent amino acids of the sequence were added by following similar steps such as activation-coupling of amino acid, end capping, and deprotection till the completion of synthesis. After addition of all the amino acids of the sequence, peptides were deprotected and cleaved from resin beads using a treatment of trifluoroacetic acid, phenol, thioanisol, 1-dodecanethiol and water (82.5:5:5:2.5:5 v/v) mixture for 4 h and precipitated in chilled dry diethyl ether.

2.2. Purification and characterization of peptides

Crude peptides were purified by reversed-phase chromatography (RP-HPLC) on a C-18 semi-preparative column (7 × 300 mm; 10 μ particle size) using UFLC pump system (Shimadzu, Tokyo, Japan) fitted with photodiode array (PDA) detector. The binary gradient solvent, water and acetonitrile having 0.1% TFA (v/v) was used for purification of peptides. The specific peaks were collected and were dried in Speed-Vac concentrator (Eppendorf, Germany) and resuspended in HPLC grade water. Eluted peptides were further analyzed on an analytical C-18 column (4 × 150 mm; 5 μ particle size). The identity and purity of the final products were confirmed by Ettan^{TM} MALDI–TOF (matrix-assisted laser desorption ionization-time-of-flight) MS (Amersham Biosciences). The physicochemical properties of the peptides were analyzed with the ProtParam algorithm at ExPASy (the Expert Protein Analysis System) provided by the Swiss Institute of Bioinformatics (SIB) (Table 1).

2.3. CD spectroscopy for secondary conformation of peptides

To elucidate the conformation of nAChRα1-subunit peptides, the CD spectroscopy was carried out using a Jasco J-810 CD spectropolarimeter (Jasco Corp, Japan). Spectra of the peptides (0.1 mg mL^{-1}) were recorded in the far-UV region (190–250 nm) with a path length of 1 mm, step resolution of 0.1 nm, at a speed of 100 nm s^{-1}, 1 s response time and a bandwidth of 1 nm. The CD contributions of water/solvents were subtracted from each spectrum. Each spectrum was recorded as an average of four scans with continuous mode. The mean residue ellipticity [θ] (in deg cm^2 dmol^{-1}) was calculated as [θ] = 100 ψ/cl, where ψ is the observed ellipticity in milli degree, c is the concentration of the sample in mollitre^{-1}, and l is the optical path length of the cell in cm. The CD machine

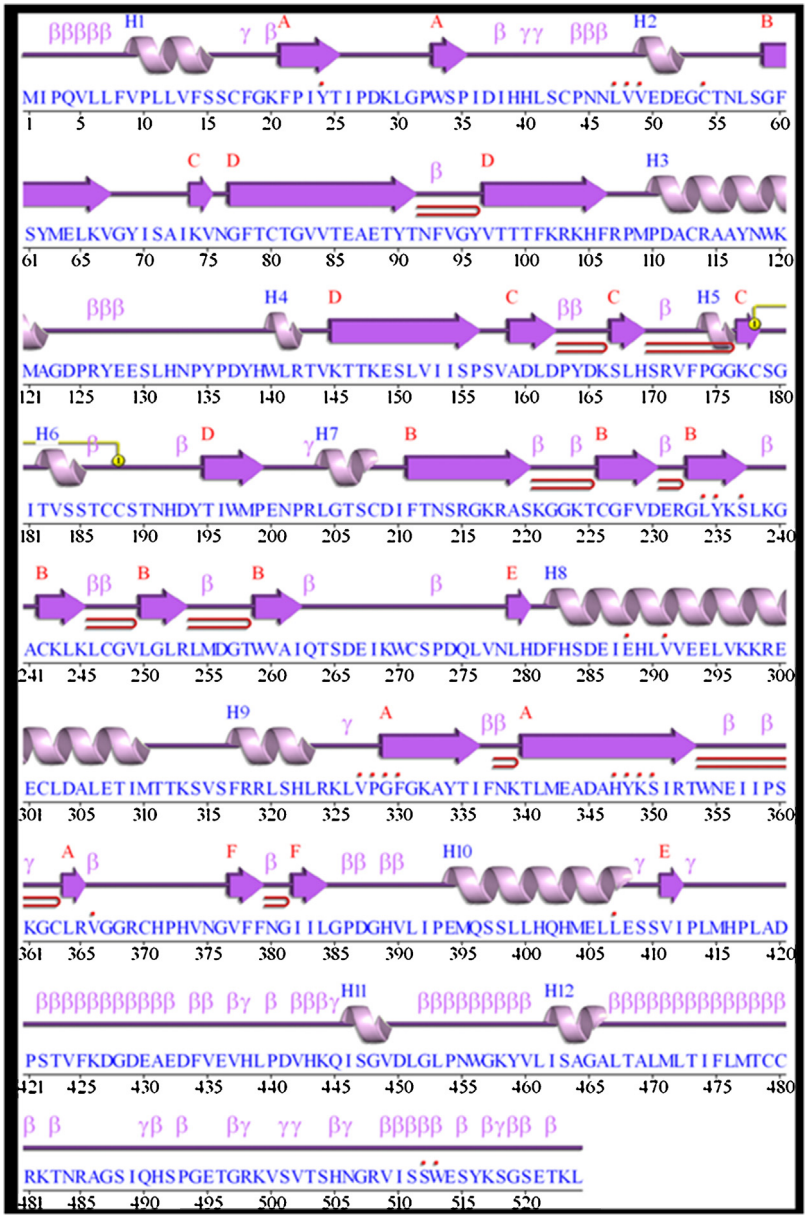

Fig. 2. Schematic diagram showing the secondary structural elements in the RABVG; α-helices are labeled with the letter "H", and β-strands are lettered in uppercase. β, γ, and hairpin turns are also labeled. (The secondary motif map and topology diagram were calculated using the PDBsum tool).

Table 1
Physico-chemical properties of nAChRα1 peptides.

Peptides	Sequence	M.Wt (g/mol)	Ex.coeff 280 nm (M^{-1} cm^{-1})	pI	Net charge at pH7
T-32	SGEWVMKDYRGWKHWVYYTCCPDTPYLDITYH	4014	23470	7.15	+0.1
C-32	SGEWVIKESRGWKHWVFYACCPSTPYLDITYH	3859	20910	8.25	+1.1
H-32	SGEWVIKESRGWKHSVTYSCCPDTPYLDITYH	3758	15220	7.16	+0.1

was calibrated using the standard solution of ammonium d-10-camphor sulfonate. The computer simulation of CD spectra was used to provide the quantitative estimation of different secondary structures of the designed peptides in solution using Spectra Manager software. The CD spectra were recorded in HPLC grade water and different concentrations of trifluoroethanol (TFE) were used to mimic the extracellular matrix and membrane environment respectively.

2.4. RABVG sequence analysis

The amino acid composition of the RABVG (ACF35025.1) was computed using the PEPSTATS analysis tool [15]. The physicochemical parameters such as the molecular weight, isoelectric point (pI), aliphatic index, amino acid property, extinction coefficient, half-life instability index, and grand average hydropathy (GRAVY) were calculated using the ProtParam tool of the ExPASy proteomics server [16]. N-glycosylation sites of the RABVG sequence were evaluated by using the NetNglyc 4.0 [17]. Sub-cellular localization of the

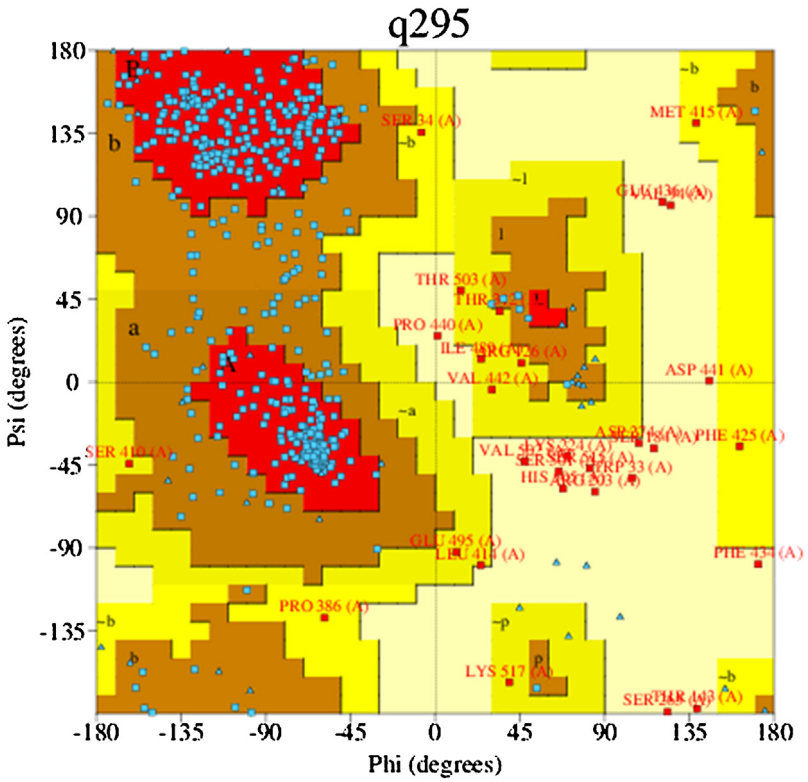

Fig. 3. Ramachandran plot of modeled structure validated by PROCHECK program.

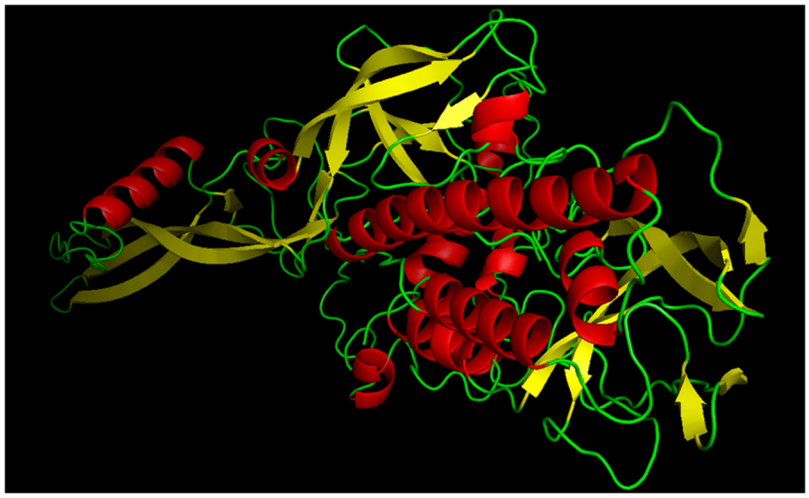

Fig. 4. Predicted structure of RABVG by I-TASSER tool showing helix, beta sheets and beta turns in red, yellow and green color respectively. (For interpretation of the references to colour in this figure legend, the reader is referred to the web version of this article.)

protein was carried out by CELLO v.2.5 (subCELlularLOcalization predictor) [18].

2.5. Structure prediction and functional annotation of RABVG

PDBsum tool was employed for calculating the secondary structural features of RABVG. The experimental 3D structure of RABVG has not been determined till now. The *de novo* method was used to develop 3D models RABVG using I-TASSER server. Model evaluation was performed by PROCHECK server for Ramachandran plot [19], Verify3D [20], ERRAT [21] is performed for validation. PyMOL (Schrödinger Inc.) was used to generate images of the RABVG model.

2.6. Molecular docking

All the *in silico* protein-chemical docking analyses were performed by using of PatchDock [22]. This server was applied to recognize the binding scores and binding residues of RABVG and nAChRα1 peptides, that were treated as a rigid body. To yield good molecular shape complementary with high competency, this method engaged 3D transformations driven by local characteristic matching and spatial pattern detection techniques, such as the geometric hashing and poses clustering. After the fast transformational search, the best geometric fit obtained the highest scores, while the low scores exhibited poor matches. Clustering RMSD was chosen as 4.0 Å and the server was applied to recognize the binding scores

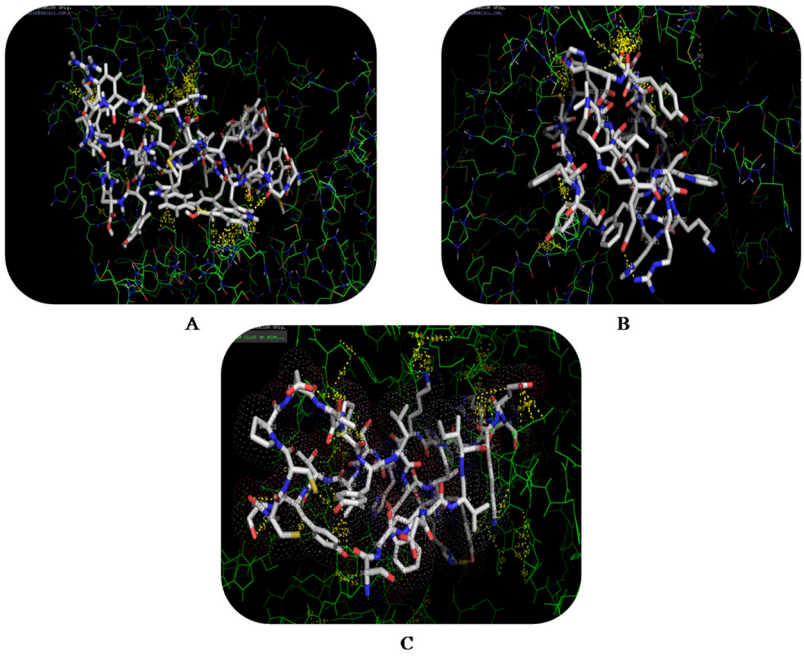

Fig. 5. Molecular docking performed to show interaction between C-32 (A), T-32 (B) and H-32 (C) nAChRα1 peptides with RABVG as visualized in pymol.

and binding residues of nAChRα1 peptides against RABVG. The PatchDock docking results were obtained and the binding affinity of peptides to RABVG are presented as docking scores.

2.7. Virus binding assay

Peptide binding to the virus was determined using standard enzyme-linked immunosorbent assay (ELISA) protocol. Peptides (100 μg/mL) were coated in the microtitre plates for 24 h at 4 °C. Blocking of empty sites was done with 1% BSA in Tris-buffered saline (TBS) for1 h at room temperature. Each well was added with 10 μg per well of β-propiolactone (BPL) inactivated RABV and incubated for 2 h at room temperature. Extensive washing was done with PBS to remove unbound virus. Wells were probed with 1:1000 dilution of monoclonal mouse anti-rabies IgG (Rab sc-57994, Santa Cruz) for 1 h at 37 °C. Chicken anti-mouse HRP conjugate (sc-2954, Santa Cruz) was added to each well, incubated for 1 h at 37 °C. The wells were washed with PBS and developed by using TMB substrate (Amresco) at room temperature for 20 min. Plates were read at 450 nm after addition of stopping solution (1 M H_2SO_4). The binding was calculated by determining the change in virus binding compared to the wells coated with BSA alone.

2.8. Peptide-mediated virus inhibition assay

Standard rapid fluorescent focus inhibition test (RFFIT) was followed to determine nAChRα1 subunit mediated inhibition of RABV infection in neuroblastoma (N2A) cells. N2A cells were grown in 24 well culture plates to reach 70–80% confluence. RABV (CVS18 strain) treated with different concentrations (5 μM to 50 μM) of nAChRα1 peptides inoculated on N2A cells by adsorption for 1hr at 37°C. The inoculum was removed and cells were incubated in under proper growth conditions. The culture media removed after 48 h post infection (hpi) and infected cell monolayers were fixed with 80% acetone followed by detection of infected cells by direct immunofluorescence test using FITC labeled antibody against RABV nucleocapsid protein (BioRad). Prolong gold anti-fade reagent with DAPI (Invitrogen) was used to counterstain the cell nuclei.

3. Results

3.1. Secondary structures of nAChRα1 peptides

In aqueous conditions, CD spectra of 32-mer peptide sequences obtained from the torpedo, bovine and human had dominant negative minimum around 195 nm with cross over to positive band at around 225 nm. Peptides were dissolved in a membrane- mimicking micro-environment by adding increasing concentrations of TFE. A marked increase in the molar ellipticity was observed at a higher concentration of TFE (>75%), indicating the increase in ordered conformations (Fig. 1). The results of the CD spectra recorded indicated the presence of alpha helix conformation of peptides in the membrane-mimicking environment. The spectra data and molar ellipticity were further analyzed using spectra manager software for quantitative estimation of the different secondary conformation of the peptides (Table 2).

3.2. Analysis of RABVG sequence

The primary structure analysis of RABVG showed that the most abundant amino acid is leucine (9.5%) and the least abundant amino acid is tryptophan (1.7%). The computed isoelectric point (pI) was 7.56 indicating that RABVG is likely to precipitate in acidic buffers. The extinction coefficient (EC) of RABVG was 74465. The instability indices (Ii) of RABVG was 34.39, which was below 40, this classifies it as stable protein. RABVG has negative GRAVY scores of −0.164 units attesting to their solubility in hydrophilic solvents. The aliphatic index (Ai) which evaluates the relative volume occupied by the side chains of hydrophobic amino acids was generally higher in the glycoprotein. A high aliphatic index indicates that a protein may remain stable over a wide range of temperatures. Glycosylation is the most abundant and diverse posttranslational modification of proteins. The NetOGlyc predicted 4 sites of glycosylation for RABVG (at positions: 179,189, 220 and 314aa).

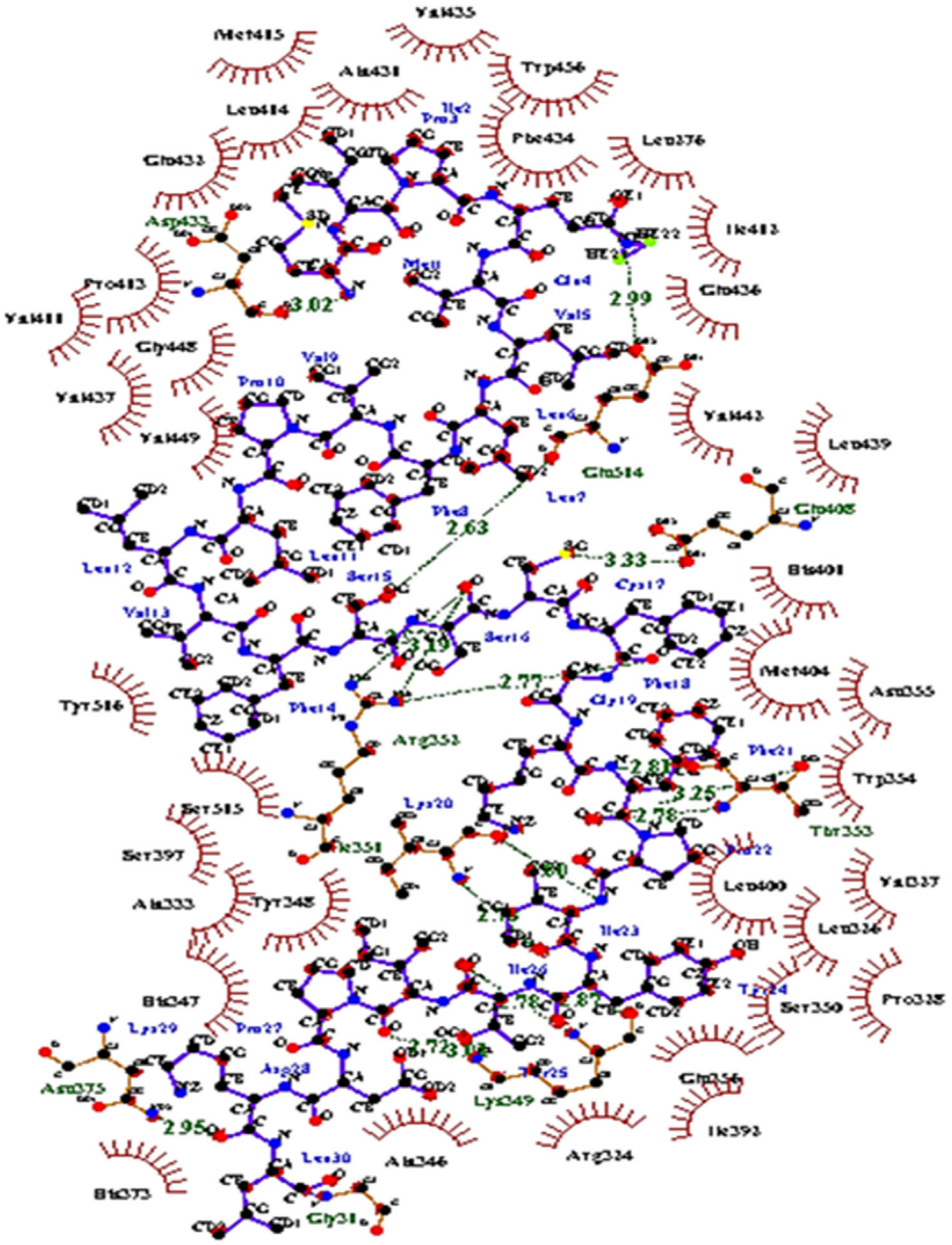

Fig. 6. Schematic diagram of interactions between C-32 and the modeled RABVG generated by LIGPLOT+. Amino acid residues are represented by three letter codes in black and blue are for RABVG and ligand, respectively. Atoms of carbon, oxygen and nitrogen are indicated by small closed circles in black, red and blue, respectively. Hydrogen bonds are indicated by green broken lines. (For interpretation of the references to colour in this figure legend, the reader is referred to the web version of this article.)

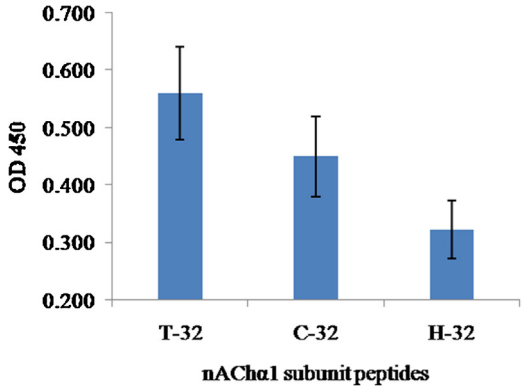

Fig. 7. Interactions of nAChRα1-subunit peptides with RABV determined by virus binding ELISA. Binding was calculated after determining the change in absorbance in virus added wells over BSA alone. Triplicates of two independent experiments were used for plotting the results (values represent Mean ± SD).

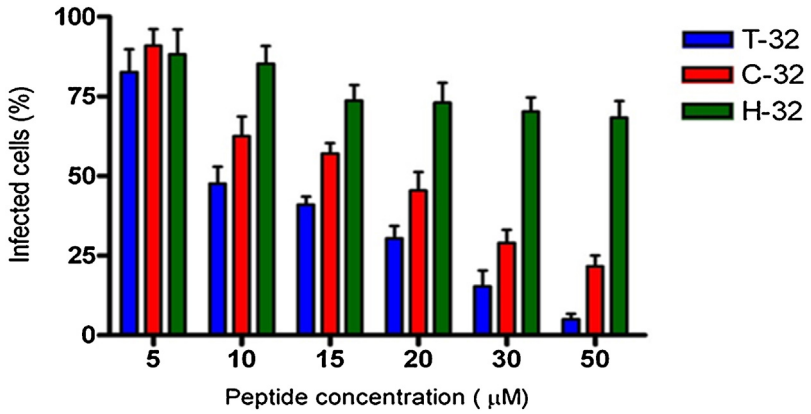

Fig. 8. Antiviral effect of nAChRα1-subunit peptides against RABV determined by rapid fluorescent focus inhibition test (RFFIT). Triplicates of each concentration of peptides were tested and the results of percentage infected cells were plotted (values represent Mean ± SD).

Table 2
Quantitative estimation of secondary structures of peptide sequences.

	In water			In 10% TFE			In 25% TFE			In 50% TFE			In 75% TFE		
	T-32	C-32	H-32	T-32	C-32	H-32	T-32	C-32	H-32	T-32	C-32	H-32	T-32	C-32	H-32
Alpha helix	0.0	0.0	0.0	0.0	0.0	0.0	0.0	67.1	0.0	25.3	100.0	20.3	83.1	100.0	76.2
Beta Sheet	0.0	0.0	0.0	0.0	0.0	0.0	0.0	0.0	0.0	0.0	0.0	0.0	0.0	0.0	0.0
Turn	0.0	0.0	70.4	0.0	0.0	48.5	0.0	0.0	0.0	0.0	0.0	0.0	0.0	0.0	0.0
Random coil	100.0	100.0	29.6	100.0	100.0	51.5	100.0	32.9	100.0	74.7	0.0	79.7	16.9	0.0	23.8

Table 3
Docking energy Score for peptides against RABVG.

Protein target	Ligand	Score	Area	ACE	Transformations
Rabies virus glycoprotein (RABVG)	T-32	13704	1790.60	−369.59	2.72 −0.83 −1.43 164.09 115.25 159.29
	C-32	14146	2144.00	−883.91	1.04 0.59 −0.21 109.97 114.76 59.13
	H-32	13180	1959.20	−453.91	−1.65 0.02 −1.26 66.46 128.97 155.13

3.3. Predicted structure of RABVG

The secondary structure composition of RABVG was determined using the PDBsum tool. The secondary structure prediction server revealed that 25.5% of amino acids resided in α-helices, while 19.3% of residues were in β-sheets (Fig. 2). The rest of the amino acids were found in other conformations such as β-hairpins and β-turns. The 3D structure of RABVG was generated using I-TESSAR server. In this method, the target sequences are first threaded using a representative PDB structure library to search for the possible folds by Profile- Profile Alignment (PPA), PSI-BLAST profiles, Hidden Markov Model, Needleman-Wunch and Smith-Waterman alignment algorithms. I-TASSER server predicted five 3D structure models from which the model with best C-Score of 2.0 was selected with estimated accuracy of 0.99 ± 0.03 (TM-Score) and 3.3 ± 2.3 Å (RMSD). C-score is a confidence score for estimating the quality of predicted models by I-TASSER server. It is calculated on the basis of the significance of threading template alignments and the convergence parameters of the structure assembly simulations. Validation of the model including the geometric properties of the backbone conformations was analyzed using various structure evaluation programs. Ramachandran plot calculations determined with PROCHECK program indicated 80.1% residues in most favored regions, 17.9% residues in the additionally allowed region with no residues in generously allowed region and 0.4% residues are in disallowed region (Fig. 3). These results revealed that the majority of the amino acids are in a phi-psi distribution that is consistent with a right-handed α-helix and the model is reliable and stable. ERRAT and Verify3D confirm the quality of predicted 3D structure by I-TASSER as more reliable and within an accepted range. The final model predicted by I-TASSER was visualized by pymol algorithm (Fig. 4).

3.4. Peptide docking to RABVG

Molecular docking was performed to predict ligand conformation and orientation at the binding site of RABVG. The docking scores on comparison indicate the best docking candidates with the RABVG (Table 3). PatchDock is a geometry-based molecular docking algorithm. It is aimed at finding docking transformations that yield good molecular shape complementarity. Such transformations, when applied, induce both wide interface areas and small amounts of steric clashes. A wide interface is ensured to include several matched local features of the docked molecules that have complementary characteristics. The Patch Dock algorithm divides the Connolly dot surface representation of the molecules into concave, convex and flat patches. Then, complementary patches are matched in order to generate candidate transformations. Each candidate transformation is further evaluated by a scoring function that considers both geometric fit and atomic desolvation. The docking results generated and depicted using pymol (Fig. 5). As indicated by results, the docking score for the B-32 and T-32 are close enough and hence represents their maximum activity against the RABVG. To understand more these two candidate's structures were superimposed at the ligand site of the RABVG. The groups involved in the interactions between the RABVG and C-32 peptide which has highest docking score generated using LIGPLOT^{+}. The results show the involvement of specific aromatic amino acids of C-32 ligand peptide (Tyr-201, Trp-207 and Tyr-209) in binding to the RABVG (Fig. 6).

3.5. Binding of nAChRα1-subunit peptides to RABV

The interactions study by virus capture ELISA indicated that the nAChRα1-subunit peptides bind to the RABV. Peptide-coated wells with higher absorbance indicated the capture of virus compared to the control wells without peptides. The torpedo peptide sequence (T-32) had the highest affinity followed by the bovine (C-32) and human (H-32) sequences (Fig. 7).

3.6. Anti-rabies effect of nAChRα1-subunit peptides

The results of the virus inhibition assay indicated that nAChRα1-subunit peptides reduced RABV infection in neuronal cells. The peptides pre-treated groups showed the reduction in the fluorescent focus units (FFU) (percentage of infected cells) compared to the untreated control groups, indicating the inhibition of RABV in N2A cells. As the peptide concentration was increased the number of RABV infected cells reduced in case of T-32 and C-32 peptides. The highest inhibition was observed in the T-32 peptide with almost negligible number of RABV infected cells at 50 μM peptide concentrations. The C-32 peptide had relatively lower effect, whereas the H-32 peptide showed no inhibition even at 50 μM concentrations (Fig. 8).

4. Discussion

Heteropentameric nAChRs are expressed by both neuronal and non-neuronal cells throughout the body and are made up of two α-subunits and one each of β, δ, and γ [23]. One essential structural feature of the α-subunits is the presence of Cys–Cys pair near the entrance of the transmembrane domain. This part represents binding site for ligands such as nicotine and neurotoxins (α-bungarotoxin) [24]. In the present study, the selected peptide sequences include Cys–Cys pair and its adjacent regions. The conformational analysis using CD spectroscopy indicated that the peptides had random coil configurations in aqueous environment. However in the membrane mimicking apolar solvent (TFE), the peptides acquired more ordered conformation. Earlier CD studies of human α1 subunit extracellular domains (ECD) recorded characteristic secondary structure composition (39% β-sheet, 22% β-turn, 4% α-helix, 33% unordered) [25]. The differences might be due to shorter length of sequences used in our study compared to the entire α1 subunit conformation. Structural studies are essential to identify groups interacting with the potential ligands. Crystal structures of nAChR revealed the specific features of ligand binding by the Cys-loop at atomic resolution and its importance in drug design for neuronal disorders [26,27]. In all these studies, nAChR structure is considered as a drug target, however, in our present study, the binding site of nAChR α1 subunit in the form of peptides are considered as ligands to target RABVG.

RABVG is mainly responsible for entry of RABV into neuronal cells (neurotropism) and *trans*-synaptic spread within the central nervous system. RABVG is a 65 kDa (524 amino acids) protein with four domains: signal peptide (SP), ectodomain (ED), transmembrane (TM), and a cytoplasmic domain (CD). Knowing the 3D structure of RABVG is important to understand its role in pathogenesis including identification drug targets. However, crystal structure of RABVG is not available and its experimental 3D structure has not yet been elucidated. Earlier studies used homology modeling for RABVG structure prediction to identify potential drug targets [28]. However, homology modeling may not yield accurate structure as the available templates crystals (2CMZ) have less sequence similarity with the RABVG (23%). Instead of homology modeling, the present study employed de novo method to accurately determine the RABVG structure using I-TESSAR server. The best 3D structure model with a C-score of 2.0 and accuracy of 0.99 ± 0.03 was obtained. The interaction of RABVG binding domains with host cell receptors such as nAChR, p75TR and NCAM is an essential step of infection [9,13]. One such interaction involves RABVG binding to the α1 subunit of nAChR [10]. In the present study, the dockings of the nAChRα1-subunit peptide sequences of different lengths between 193aa to 224aa, derived from three different species (torpedo, bovine, human) were done using PatchDock algorithm. The highest docking scores of C-32 followed by T-32 peptides indicated the role of non-conservative aromatic amino acids (Tyr-201, Trp-207 and Tyr-209) within nAChRα1-subunit peptides. Earlier studies have indicated that RABV interacts with α1-subunit of the nAchR from torpedo electric organ membranes and competes with bungarotoxin [10,11]. In our peptide-virus interaction studies, the maximum reactivity was observed for T-32 followed by C-32.

The binding of receptor origin peptides to virus glycoprotein may prevent entry of virus particles into host cells potentially preventing the infection [29]. In the present study, selected nAChRα1subunit peptides reduced the rabies infections in cultured neuronal cells. The dose-dependent inhibition RABV by the peptides indicated their potential antiviral properties. Peptide antivirals designed to target different regions of rabies phosphoprotein (P) inhibited RABV multiplication [30,31]. Host and virus protein–protein interactions were screened to design and develop potential antiviral drugs against RABV [32]. It may be possible that the peptides used in the present study may function like rabies immunoglobulins (RIG) to prevent rabies infection.

5. Conclusions

In the present study, RABVG binding site was predicted and docking analysis was done. Docking studies revealed that nAChRα1 peptides, T-32 and C-32 pose perfect fit in the binding site of the RABVG. The peptides show similar overlapping regions within the binding site. The experiments indicated that even though both C-32 and T-32 peptide shown virus binding properties, T-32 was more efficient in inhibiting the RABV infection. However further studies on improved designs for higher binding capacity and ability to enter neurons are warranted to develop these peptides as potential antiviral agents for RABV.

Conflict of interest

The authors declare that there is no conflict of interest regarding this work.

Acknowledgement

We are thankful to the Director, IVRI, Izatnagar, Bareilly, UP-243122, India for providing all the necessary facilities to conduct research.

References

[1] WHO Expert Consultation on Rabies, Second Report WHO technical report series; no. 982, (2013).
[2] H. Wilde, T. Hemachudha, The Milwaukee protocol for treatment of human ra-Rabies is no longer valid, Pediatr. Infect. Dis. J. 34 (2015) 678–679.
[3] A.S. Huang, W.C. Chen, W.T. Huang, S.T. Huang, Y.C. Lo, S.H. Wei, H.W. Kuo, P.C. Chan, M.N. Hung, Y.L. Liu, J.J. Mu, J.Y. Yang, D.P. Liu, J.H. Chou, J.H. Chuang, F.Y. Chang, Public health responses to reemergence of animal rabies, Taiwan PLoS ONE 10 (2015) e0132160.
[4] K. Muhamuda, S.N. Madhusudana, V. Ravi, Use of neutralizing murine monoclonal antibodies to rabies glycoprotein in passive immunotherapy against rabies, Hum. Vaccine 5 (2007) 192–195.
[5] A.B. Bakker, C. Python, C.J. Kissling, P. Pandya, W.E. Marissen, M.F. Brink, F. Lagerwerf, S. Worst, E. van Corven, S. Kostense, K. Hartmann, G.J. Weverling, F. Uytdehaag, C. Herzog, D.J. Briggs, C.E. Rupprecht, R. Grimaldi, J. Goudsmit,

First administration to humans of a monoclonal antibody cocktail against rabies virus: safety, tolerability, and neutralizing activity, Vaccine 26 (2008) 5922–5927.
[6] A.M.Q. King, M.J. Adams, E.B. Carstens, E.J. Lefkowitz, Virus Taxonomy: Classification and Nomenclature of Viruses: Ninth Report of the International Committee on the Taxonomy of Viruses, Elsevier Academic Press, CA, San Diego, 2012.
[7] S. Finke, K.K. Conzelmann, Replication strategies of rabies virus, Virus Res. 111 (2005) 120–131.
[8] S. Roche, Y. Gaudin, Evidence that rabies virus forms different kinds of fusion machines with different pH thresholds for fusion, J. Virol. 78 (2004) 8746–8752.
[9] M. Lafon, Rabies virus receptors, J. Neurovirol. 11 (2005) 82–87.
[10] M. Gustka, J. Horvat, L.T. Lentz, Rabies virus binding to the nicotinic acetylcholine receptor (subunit demonstrated by the virus overlay protein binding assay, J. Gen.Virol. 77 (1996) 2437–2440.
[11] T.L. Lentz, The recognition event between virus and host cell receptor: a target for antiviral agents, J. Gen. Virol. 71 (1990) 751–756.
[12] M. Rustici, L. Bracci, L. Lozzi, P. Neri, A. Santucci, P. Soldani, A. Spreafico, N. Niccolai, A model of the rabies virus glycoprotein active site, Biopolymers 33 (1993) 961–969.
[13] M.J. Schnell, J.P. McGettigan, C. Wirblich, A. Papaneri, The cell biology of rabiesvirus: using stealth to reach the brain, Nat. Rev. Microbiol. 8 (2010) 51–61.
[14] E. Kaiser, R.L. Colescott, C.D. Bossinger, P.I. Cook, Color test for detection of free terminal amino groups in the solid-phase synthesis of peptides, Anal. Biochem. 34 (1970) 595–598.
[15] P. Rice, I. Longden, A. Bleasby, EMBOSS the European molecular biology open software suite, Trends Genet. 16 (2000) 276–277.
[16] E. Gasteiger, A. Gattiker, C. Hoogland, I. Ivanyi, R.D. Appel, A. Bairoch, ExPASy the proteomics server for in-depth protein knowledge and analysis, Nucleic Acids Res. 31 (2003) 3784–3788.
[17] R. Gupta, S. Brunak, Prediction of glycosylation across the human proteome and the correlation to protein function, Pac. Symp. Biocomput. (2002) 310–322.
[18] C.S. Yu, C.J. Lin, J.K. Hwang, Predicting subcellular localization of proteins for gram-negative bacteria by support vector machines based on n-peptide compositions, Protein Sci. 13 (2004) 14021406.
[19] R.A. Laskowski, M.W. MacArthur, D.S. Moss, J.M. Thronton, PROCHECK. a program to check the stereochemical quality of protein structures, J. Appl Cryst. 26 (1993) 283–291.
[20] D. Eisenberg, R. Luthy, J.U. Bowie, VERIFY3D: assessment of protein models with three-dimensional profiles, Methods Enzymol. 277 (1997) 396–404.
[21] C. Colovos, T.O. Yeates, Verification of protein structures: patterns of nonbonded atomic interactions, Protein Sci. 2 (1993) 1511–1519.
[22] D. Schneidman-Duhovny, Y. Inbar, R. Nussinov, H.J. Wolfson, PatchDock and SymmDock: servers for rigid and symmetric docking, Nucl. Acids. Res. 33 (2005) 363–367.
[23] C. Gotti, F. Clementi, Neuronal nicotinic receptors: from structure to pathology, Prog. Neurobiol. 74 (2004) 363–396.
[24] E.X. Albuquerque, E.F. Pereira, M. Alkondon, S.W. Rogers, Mammalian nicotinic acetylcholine receptors: from structure to function, Physiol. Rev. 89 (2009) 73–120.
[25] M. Zouridakis, K. Kostelidou, A. Sotiriadis, C. Stergiou, E. Eliopoulos, K. Poulas, S.J. Tzartos, Circular dichroism studies of extracellular domains of human nicotinic acetylcholine receptors provide an insight into their structure, Int. J. Biol. Macromol. 41 (2007) 423–429.
[26] C.D. Dellisanti, Y. Yao, J.C. Stroud, Z.Z. Wang, L. Chen, Crystal structure of the extracellular domain of nAChR alpha1 bound to alpha-bungarotoxin at 1.94 A resolution, Nat. Neurosci. 10 (2007) 953–962.
[27] K. Lazaridis, P. Zisimopoulou, P. Giastas, K. Bitzopoulou, P. Evangelakou, A. Sideri, S.J. Tzartos, Expression of human AChR extracellular domain mutants with improved characteristics, Int. J. Biol. Macromol. 63 (2014) 210–217.
[28] N.R. Tomar, V. Singh, S.S. Marla, R. Chandra, R. Kumar, A. Kumar, Molecular docking studies with rabies virus glycoprotein to design viral therapeutics, Indian J. Pharm. Sci. 72 (2010) 486–490.
[29] E. Teissier, F. Penin, E.I. Pécheur, Targeting cell entry of enveloped viruses as an antiviral strategy, Molecules 16 (2011) 221–250.
[30] E. Real, J.C. Rain, V. Battaglia, C. Jallet, P. Perrin, N. Tordo, P. Chrisment, J. D'Alayer, P. Legrain, Y. Jacob, Antiviral drug discovery strategy using combinatorial libraries of structurally constrained peptides, J. Virol. 78 (2004) 7410–7417.
[31] G. Castel, M. Chtéoui, G. Caignard, C. Préhaud, S. Méhouas, E. Réal, C. Jallet, Y. Jacob, R.W. Ruigrok, N. Tordo, Peptides that mimic the amino-terminal end of the rabies virus phosphoprotein have antiviral activity, J. Virol. 83 (2009) 10808–10820.
[32] U.F. Lingappa, X. Wu, A. Macieik, S.F. Yu, A. Atuegbu, M. Corpuz, J. Francis, C. Nichols, A. Calayag, H. Shi, J.A. Ellison, E.K. Harrell, V. Asundi, J.R. Lingappa, M.D. Prasad, W.I. Lipkin, D. Dey, C.R. Hurt, V.R. Lingappa, W.J. Hansen, C.E. Rupprecht, Host–rabies virus protein–protein interactions as druggable antiviral targets, Proc. Natl. Acad. Sci. U. S. A. 110 (2013) E861–E868.